# Tunable Capacitor For Superconducting Qubits Using an InAs/InGaAs Heterostructure

## C30: I/O, Packaging, & 3D Integration for Superconducting and Semiconductor Qubits I

Nick Materise[1], Matthieu Dartiailh[2], Javad Shabani[2], Eliot Kapit[1]

[1]Colorado School of Mines, Department of Physics

[2]Center for Quantum Phenomena, Department of Physics, New York University

March 15, 2021

COLORADO SCHOOL OF MINES
EARTH • ENERGY • ENVIRONMENT

# Voltage vs. Flux Biased Couplers

## Voltage-controlled coupler[1]

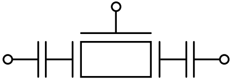

## Flux-tunable coupler[2]

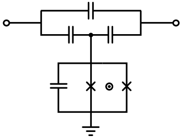

[1] See A37.00009, P29.00013

[2] Adapted from J. Martinis, SQuInT 2020

# Voltage vs. Flux Biased Couplers

## Voltage-controlled coupler[1]

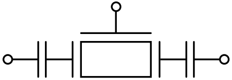

+ 2nd order sensitive to voltage bias
+ No heating introduced by voltage bias
+ Minimal cross-talk expected

## Flux-tunable coupler[2]

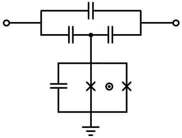

- 1st order sensitive to flux bias
- Current biases can heat system
- Cross-talk from stray magnetic fields

[1] See A37.00009, P29.00013

[2] Adapted from J. Martinis, SQuInT 2020

# Voltage vs. Flux Biased Couplers

## Voltage-controlled coupler[1]

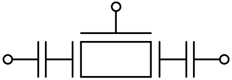

- + 2nd order sensitive to voltage bias
- + No heating introduced by voltage bias
- + Minimal cross-talk expected
- - Not part of cQED fab, yet
- - Dielectric loss from 2DEG possible

## Flux-tunable coupler[2]

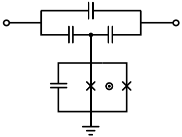

- - 1st order sensitive to flux bias
- - Current biases can heat system
- - Cross-talk from stray magnetic fields
- + Compatible with cQED fab
- + Loss from distributed capacitors

[1] See A37.00009, P29.00013

[2] Adapted from J. Martinis, SQuInT 2020

# Device Design & Semiconductor Simulations

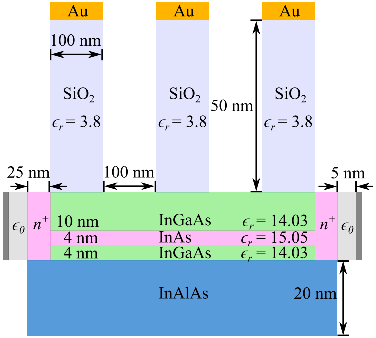

# Device Design & Semiconductor Simulations

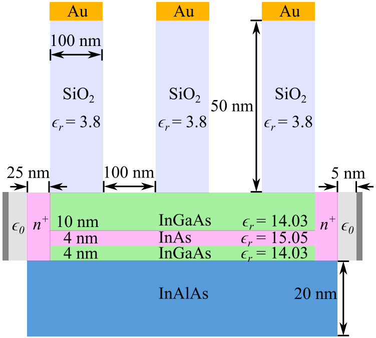


- Electron densities calculated from equilibrium solutions to the drift-diffusion equations with Fermi-Dirac statistics in COMSOL
- 2DEG confinement included with density gradients modifying the equilibrium electron densities[3]
- Electrostatic charge conservation applied to InAlAs, $SiO_2$, and air-gap dielectric regions

[3] Ancona, Journal of Computational Electronics **10**, 65 (2011).

# Device Design & Semiconductor Simulations

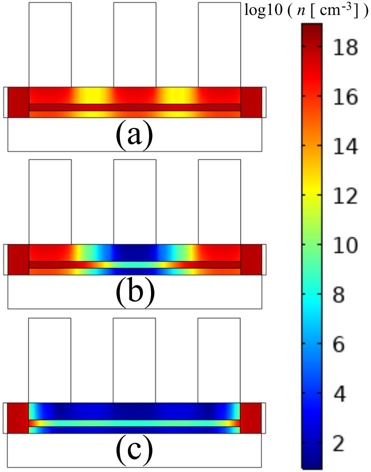


- Electron densities calculated from equilibrium solutions to the drift-diffusion equations with Fermi-Dirac statistics in COMSOL
- 2DEG confinement included with density gradients modifying the equilibrium electron densities[3]
- Electrostatic charge conservation applied to InAlAs, $SiO_2$, and air-gap dielectric regions
- Electron densities for three gate configurations

[3] Ancona, Journal of Computational Electronics **10**, 65 (2011).

# Capacitance Matrix DC Calculations

- Simplify geometry into perfect electric conductors and ideal dielectrics in the fully conducting / depleted limits of the 2DEG
- End-to-end capacitance limited by air-gap capacitors (enlarged to reduce aspect ratio in COMSOL simulations)

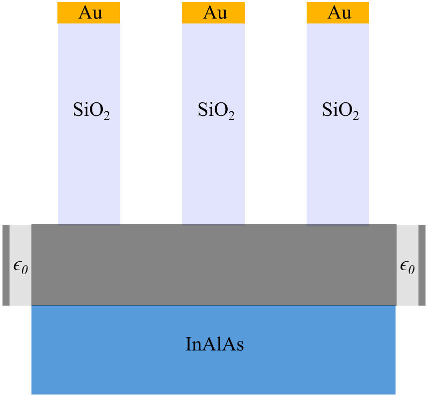


Fully Conducting

# Capacitance Matrix DC Calculations

- Simplify geometry into perfect electric conductors and ideal dielectrics in the fully conducting / depleted limits of the 2DEG
- End-to-end capacitance limited by air-gap capacitors (enlarged to reduce aspect ratio in COMSOL simulations)

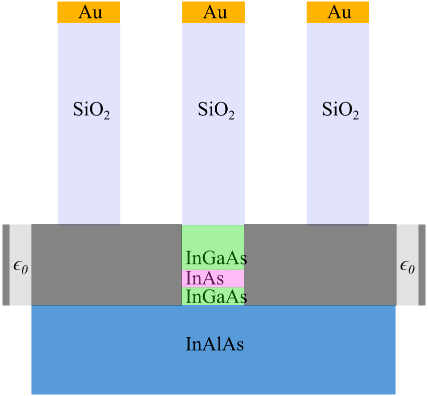


Fully Depleted Single Gate

# Capacitance Matrix DC Calculations

- Simplify geometry into perfect electric conductors and ideal dielectrics in the fully conducting / depleted limits of the 2DEG
- End-to-end capacitance limited by air-gap capacitors (enlarged to reduce aspect ratio in COMSOL simulations)

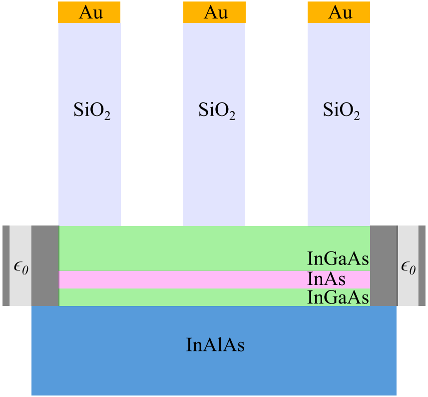


Fully Depleted Three Gates

# Capacitance Matrix DC Calculations

- Solve Poisson's equation with the charge continuity equation in 2D

$$-\nabla \cdot d\left(\varepsilon_0 \nabla V - \mathrm{P}\right) = \rho$$

- Extract Maxwell capacitance matrix

$$\begin{pmatrix} Q_1 \\ Q_2 \\ \vdots \\ Q_N \end{pmatrix} = \begin{pmatrix} C_{11} & C_{12} & \dots & C_{1N} \\ C_{21} & C_{22} & \dots & C_{2N} \\ \vdots & \vdots & & \vdots \\ C_{N1} & C_{N2} & \dots & C_{NN} \end{pmatrix} \begin{pmatrix} V_1 \\ V_2 \\ \vdots \\ V_N \end{pmatrix}$$

- On/off ratio of $C_{12}^{\mathrm{on}} \;/\; C_{12}^{\mathrm{off}} = 30.8\ \mathrm{aF} \;/\; 0.199\ \mathrm{aF} \approx 160!$

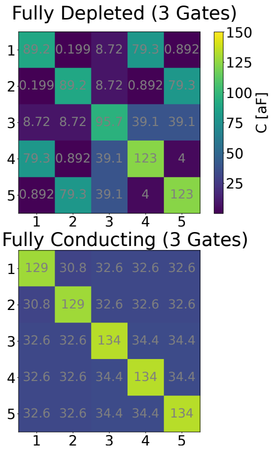

# Conductance Matrix Calculations

- Solve time harmonic equations

$$\nabla \cdot (\sigma \mathrm{E} + \mathrm{J}_e) + i\omega\rho = 0,$$
$$\nabla \cdot \mathrm{D} = \rho$$

- Use terminal current, voltage solutions to compute admittance matrix, Y

$$\begin{pmatrix} V_1 \\ V_2 \\ \vdots \\ V_N \end{pmatrix} = \begin{pmatrix} Y_{11} & Y_{12} & \dots & Y_{1N} \\ Y_{21} & Y_{22} & \dots & Y_{2N} \\ \vdots & \vdots & & \vdots \\ Y_{N1} & Y_{N2} & \dots & Y_{NN} \end{pmatrix} \begin{pmatrix} I_1 \\ I_2 \\ \vdots \\ I_N \end{pmatrix}$$
$$\mathrm{Y} = \mathrm{G} + i\omega \mathrm{C}$$

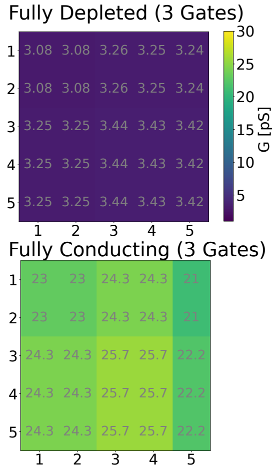

# Dielectric Loss Estimation

- Estimation of dielectric loss-limited $T_1$[4,5]

$$T_1^{-1} = \frac{\omega}{Q} = \omega \sum_j \frac{p_j}{Q_j} + \Gamma_0, \; Q_j^{-1} = \tan\delta_j$$

$$p_j = \frac{t_j \varepsilon_{1,j} \int_{S_j} |\mathrm{E}|^2 \, dS}{\int_V |\mathrm{E}|^2 dV}$$

| | $t_j$ [nm] | $p_j$ | $\tan\delta_j$ | $T_1$ [$\mu$s] |
|---|---|---|---|---|
| InGaAs | 10 | 2.08E-5 | 4.8E-5 | 3190 |
| InAs | 4 | 3.18E-5 | 4.8E-5 | 20800 |
| InGaAs | 4 | 2.86E-5 | 4.8E-5 | 23200 |
| InAlAs | 20 | 5.64E-4 | 4.8E-5 | 1180 |
| $SiO_2$[7] | 50 | 4.44E-3 | 2.00E-3 | 3.58 |
| Total | - | - | - | 3.57 |

- III-V loss tangents approximated with GaAs[6]
- Limited by $SiO_2$, pending measurement of III-Vs

[4] Wenner et al., Applied Physics Letters **99**, 113513 (2011).
[5] Wang et al., Applied Physics Letters **107**, 162601 (2015).
[6] McRae et al., arXiv e-prints, arXiv:2009.10101 (2020).
[7] Li et al., IEEE Transactions on Applied Superconductivity **23**, 1501204 (2013).

# Matrix Element Extraction – Energy Participation Ratios

Two Transmon + Coupler HFSS Model
[Insets: Junctions and Coupler Enlarged]

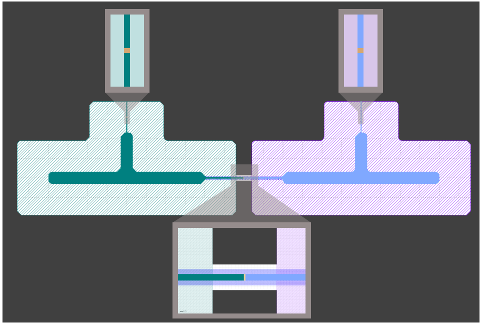

- HFSS Eigenmodes → EPR → Matrix Elements[8,9]
- Josephson junction inductances, capacitances as inputs
- Coupler modeled as lumped element capacitor

[8] Minev, arXiv e-prints, arXiv:1902.10355 (2019).

[9] Minev et al., arXiv e-prints, arXiv:2010.00620 (2020).

# Matrix Element Extraction – Energy Participation Ratios

## Two Transmon + Coupler Eigenmodes

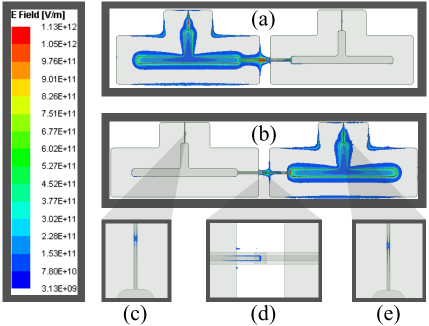


Figure: Electric field norm of first three eigenmode solutions. (a) 5.9 GHz, (b) 6.1 GHz, and (c-e) 8.6 GHz; scaled views of (c) qubit 1, (d) coupling element, and (e) qubit 2 electric field norms of third eigenmode.

- HFSS Eigenmodes → EPR → Matrix Elements[8,9]
- Josephson junction inductances, capacitances as inputs
- Coupler modeled as lumped element capacitor

[8] Minev, arXiv e-prints, arXiv:1902.10355 (2019).

[9] Minev et al., arXiv e-prints, arXiv:2010.00620 (2020).

# Matrix Element Extraction – Energy Participation Ratios

| Mode No. | $\omega/2\pi$ [GHz] | Q | | $\chi/2\pi$ [MHz] | |
|---|---|---|---|---|---|
| 1 (d) | 5.667 | 4.5E8 | **226** | 62.5 | 0.965 |
| 2 (d) | 5.838 | 1.3E9 | 62.5 | **226** | 1.11 |
| 3 (d) | 8.614 | 1.8E13 | 0.965 | 1.11 | **0.002** |
| 1 (c) | 5.669 | 4.5E8 | **223** | 67.1 | 0.974 |
| 2 (c) | 5.840 | 1.3E9 | 67.1 | **223** | 1.12 |
| 3 (c) | 8.612 | 1.8E13 | 0.974 | 1.12 | **0.002** |

Table: Extracted matrix elements from energy participation ratio calculations for values of $R_{12}$, $C_{12}$ in the fully depleted (d) and fully conducting (c) limits of the 2DEG. Diagonal entries of $\chi$ are scaled by $1/2$ to denote the anharmonicities.

- HFSS Eigenmodes → EPR → Matrix Elements[8,9]
- Josephson junction inductances, capacitances as inputs
- Coupler modeled as lumped element capacitor
- Parametric sweep over the coupler capacitance to extract self- and cross-Kerr matrix elements

[8] Minev, arXiv e-prints, arXiv:1902.10355 (2019).

[9] Minev et al., arXiv e-prints, arXiv:2010.00620 (2020).

# Matrix Element Extraction – Energy Participation Ratios

| Mode No. | $\omega/2\pi$ [GHz] | Q | | $\chi/2\pi$ [MHz] | |
|---|---|---|---|---|---|
| 1 (d) | 5.667 | 4.5E8 | **226** | 62.5 | 0.965 |
| 2 (d) | 5.838 | 1.3E9 | 62.5 | **226** | 1.11 |
| 3 (d) | 8.614 | 1.8E13 | 0.965 | 1.11 | **0.002** |
| 1 (c) | 5.669 | 4.5E8 | **223** | 67.1 | 0.974 |
| 2 (c) | 5.840 | 1.3E9 | 67.1 | **223** | 1.12 |
| 3 (c) | 8.612 | 1.8E13 | 0.974 | 1.12 | **0.002** |

Table: Extracted matrix elements from energy participation ratio calculations for values of $R_{12}$, $C_{12}$ in the fully depleted (d) and fully conducting (c) limits of the 2DEG. Diagonal entries of $\chi$ are scaled by $1/2$ to denote the anharmonicities.

- HFSS Eigenmodes → EPR → Matrix Elements[8,9]
- Josephson junction inductances, capacitances as inputs
- Coupler modeled as lumped element capacitor
- Parametric sweep over the coupler capacitance to extract self- and cross-Kerr matrix elements
- Retain anharmonicities for exchange interaction matrix elements

[8] Minev, arXiv e-prints, arXiv:1902.10355 (2019).

[9] Minev et al., arXiv e-prints, arXiv:2010.00620 (2020).

# Matrix Element Extraction – Exchange Interaction

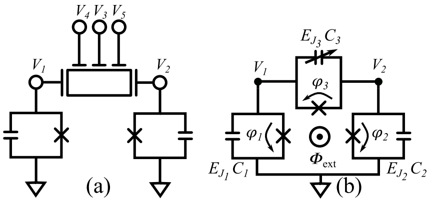


- Extract exchange $Q_i Q_j$ interaction matrix elements $C^{-1}/2$ from[10,11]

$$H = \frac{1}{2} \mathrm{Q}^T C^{-1} \mathrm{Q} + \sum_j E_{J_j} \left(1 - \cos \varphi_j\right)$$

$$C = \begin{pmatrix} C_1 + C_3 & -C_3 \\ -C_3 & C_2 + C_3 \end{pmatrix}$$

$$C_k = \frac{e^2}{2E_C} \simeq -\frac{e^2}{2\alpha_k} = -\frac{e^2}{2\chi_{kk}}$$

[10] Orlando et al., Phys. Rev. B **60**, 15398 (1999).

[11] Koch et al., Phys. Rev. A **76**, 042319 (2007).

# Matrix Element Extraction – Exchange Interaction

- Extract exchange $Q_i Q_j$ interaction matrix elements $C^{-1}/2$ from[10,11]

$$H = \frac{1}{2}\mathrm{Q}^T C^{-1}\mathrm{Q} + \sum_j E_{J_j}\left(1 - \cos\varphi_j\right)$$

$$C = \begin{pmatrix} C_1 + C_3 & -C_3 \\ -C_3 & C_2 + C_3 \end{pmatrix}$$

$$C_k = \frac{e^2}{2E_C} \simeq -\frac{e^2}{2\alpha_k} = -\frac{e^2}{2\chi_{kk}}$$

- Exchange interaction matrix elements recover $\approx$160 on/off ratio

| Qubit Index | Matrix Elements | [MHz] |
|---|---|---|
| 1 (d) | 226 | **0.0005** |
| 2 (d) | 0.0005 | 226 |
| 1 (c) | 226 | **0.079** |
| 2 (c) | 0.079 | 226 |

Table: Charge-charge (exchange) interaction matrix elements in the (d) depleting and (c) conducting limits of the 2DEG coupler.

[10] Orlando et al., Phys. Rev. B **60**, 15398 (1999).

[11] Koch et al., Phys. Rev. A **76**, 042319 (2007).

# Summary

- Capacitive couplers are drop-in replacements for their inductive counterparts
- We estimate on/off ratios of two orders of magnitude in two transmon geometry
- Dielectric loss dominated by $SiO_2$, pending experimental verification
- Opens the door for future semiconductor-superconducting hybrid systems

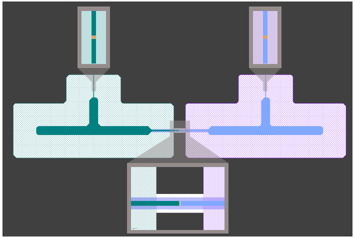

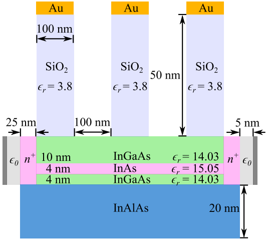

# Acknowledgements


- We acknowledge support from the Graduate Fellowships for STEM Diversity, NSF grant No. PHY-1653820, ARO grant No. W911NF-18-1-0125 and LPS/ARO grant No. W911NF-18-1-0115
- We would like to thank Joel Howard, Bradley Lloyd, Paul Niyonkuru, David Rodríguez Pérez, Zhijie Tang, Meenakshi Singh, William Strictland, and Joseph Yuan for helpful discussions

# References


[1] M. G. Ancona. "Density-gradient theory: a macroscopic approach to quantum confinement and tunneling in semiconductor devices". In: *Journal of Computational Electronics* 10.1 (June 2011), 65. DOI: 10.1007/s10825-011-0356-9.

[2] Jens Koch et al. "Charge-insensitive qubit design derived from the Cooper pair box". In: *Phys. Rev. A* 76 (4 Oct. 2007), 042319. DOI: 10.1103/PhysRevA.76.042319.

[3] D. Li et al. "Improvements in Silicon Oxide Dielectric Loss for Superconducting Microwave Detector Circuits". In: *IEEE Transactions on Applied Superconductivity* 23.3 (2013), 1501204.

[4] C. R. H. McRae et al. "Dielectric loss in epitaxial Al/GaAs/Al trilayers for superconducting circuits". In: *arXiv e-prints*, arXiv:2009.10101 (Sept. 2020), arXiv:2009.10101. arXiv: 2009.10101 [physics.app-ph].

[5] Zlatko K. Minev. "Catching and Reversing a Quantum Jump Mid-Flight". In: *arXiv e-prints*, arXiv:1902.10355 (Feb. 2019), arXiv:1902.10355. arXiv: 1902.10355 [quant-ph].

[6] Zlatko K. Minev et al. "Energy-participation quantization of Josephson circuits". In: *arXiv e-prints*, arXiv:2010.00620 (Oct. 2020), arXiv:2010.00620. arXiv: 2010.00620 [quant-ph].

[7] T. P. Orlando et al. "Superconducting persistent-current qubit". In: *Phys. Rev. B* 60 (22 Dec. 1999), 15398. DOI: 10.1103/PhysRevB.60.15398.

[8] C. Wang et al. "Surface participation and dielectric loss in superconducting qubits". In: *Applied Physics Letters* 107.16 (2015), 162601. DOI: 10.1063/1.4934486. eprint: https://doi.org/10.1063/1.4934486.

[9] J. Wenner et al. "Surface loss simulations of superconducting coplanar waveguide resonators". In: *Applied Physics Letters* 99.11 (2011), 113513. DOI: 10.1063/1.3637047. eprint: https://doi.org/10.1063/1.3637047.